Preparation and characterization of particles with small differences in polydispersity

H. J. Schöpe[1], O. Marnette[2], W. van Megen[3] and G. Bryant[3]*

[1]Institut für Physik, Johannes Gutenberg-Universität Mainz, Staudingerweg 7, D-55128 Mainz, Germany

[2]Laboratoire de Physique Statistique de l'Ecole Normale Supérieure, associé aux universitiés Paris VI et Paris VII, 24, rue Lhomond, 75231 Paris Cedex 05, France

[3]Applied Physics, Royal Melbourne Institute of Technology, Melbourne, Vic 3000, Australia

jschoepe@uni-mainz.de

RECEIVED DATE (to be automatically inserted after your manuscript is accepted if required according to the journal that you are submitting your paper to)

Small differences in polydispersity

Colloidal particles are widely used both in fundamental research and in materials science. One important parameter influencing the physical properties of colloidal materials is the particle size distribution (polydispersity) of the colloidal particles. Recent work on colloidal crystallization has demonstrated that even subtle changes in polydispersity can have significant effects. In this study we present centrifugation techniques for subtle manipulating the width and the shape of the particle size distribution, for polydispersities less than 10%. We use scanning electron microscopy as well as dynamic and static light scattering to characterize the particle size distributions. We compare the results, and highlight the difficulties associated with the determination of accurate particle size distributions.

colloids, static light scattering, dynamic light scattering, scanning electron microscopy, particle size distribution, particle sizing

Introduction

Colloidal particles are widely used as a tool to study a range of problems in fundamental science. One particular area where colloidal particles have had an impact is in the study of crystallization and the glass transition, where colloidal particles with a range of properties have been employed. These include suspensions of particles which behave as hard-spheres,[1] which have long range electrical interactions,[2] medium range magnetic interactions,[3] and short range depletion attractions (see[4,5] and references in these works). All colloidal particles have a particle size distribution, with polydispersities which can be as small as a few percent. In many applications, particles with such narrow size distributions are generally denoted as 'monodisperse'[6].

However, there are some cases where the detailed nature of the particle size distribution become exceedingly important, and characterization of the particle size distribution becomes critical. In particular it has become apparent in the past few years that subtle difference in particle size distributions can have a huge impact on colloidal self assembly – such as on crystallization in hard-spheres (see [7-12] and references therein). Indeed, it now appears that the extensive knowledge gained on crystallization and the glass transition in colloidal hard spheres has been possible partly due to fortuitous level of polydispersity inherent in these systems. The importance of polydispersity is also demonstrated by the fact that in molecular dynamics studies of hard spheres, polydispersity must be artificially introduced in order to slow crystallization and allow the investigation of metastable fluids and the glass transition.[13-15]

We have recently demonstrated that the nucleation and crystal growth processes in colloidal hard spheres are extremely sensitive to even small changes in polydispersity.[16, 17]

Polydispersity affects the type of crystalline structure as well as the crystal morphology of the resulting material. It is the main origin of bad spots, dislocations, stacking faults and unregistered plains.[17-20] These observations strongly suggest that the details of the polydispersity are critical for any applications: for example the use of colloidal crystals as a starting material for photonic band gap materials will be limited by the polydispersity, as imperfect crystal structures will reduce the width of

the band gap.

There are several techniques for characterizing particles size, including those based on scattering techniques, fractionation/filtration techniques, particle counting techniques, and microscopy – for a detailed review see,[21] which all have their advantages and disadvantages. However, most of these techniques are not suitable for the characterization of very small differences in polydispersity, or if they are suitable, have rarely been applied to what many people consider to be 'monodisperse' particles. In addition, particle size distribution measurements are weighted by factors determined by the technique used, and may not represent a "true" value. The most accurate determination of particle size distributions are achieved where more than one method of characterization is used.

Three techniques which can in principle be used to study small changes in polydispersity are scanning electron microscopy (SEM) and both Dynamic and Static Light Scattering (DLS and SLS). SEM suffers from the possibility of artefacts introduced during sample preparation, and from poor counting statistics (discussed later). DLS and SLS on the other hand have excellent statistics, but also have disadvantages: DLS suffers from the so-called inversion problem - the particle size distribution is obtained by the numerical inversion of a Laplace transform, to which there is no unique solution; and SLS suffers from low information content. A range of techniques have been developed to improve the results by combining the two methods (eg see [22-25] and references in those works). For small polydispersities, a simpler method can be used.[26, 27]

In order to study the effects of these small changes in the particle size distribution on crystallization in hard-sphere suspensions, it has been necessary to develop methods to prepare and characterize suspensions with subtle differences in polydispersity. In this paper we present the results of these investigations. First, we show how subtle changes in polydispersity can be achieved by fractionation techniques, and we apply these technique to both sub-micronic and micronic sized particles (suitable for light scattering and visible light microscopy respectively). Second we investigate particle size distribution determination using Scanning Electron Microscopy (SEM), and discuss the importance of

sample preparation to avoid local fractionation during drying, as well as investigating the number of particles needed to obtain good statistics. Third we compare these results with both Dynamic Light Scattering (DLS) and Static Light Scattering (SLS) methods.

Experimental

Two different particle suspensions are used here, one (~320nm radius) designed for use in light scattering experiments, and one (~1360nm radius) designed for light microscopy experiments. Particles of both types have been widely used for studies of phase transitions in hard-spheres. The particles are prepared by emulsion polymerization and consist of a either a polymer core of methylmethacrylate (MMA), or a copolymer core of MMA and tri-fluoroethylacrylate (TFEA). In both cases the particles are stabilised with a coating of poly-12-hydroxystearic acid (PHSA) bonded to the surface. This coating is between 10 and 15nm thick, depending on the particles,[28] and gives the particles their hard sphere character when suspended in appropriate solvents, as demonstrated by direct measurements.[29] For phase transition studies at high concentrations in 3D, the refractive indices of the particles and solvent must be closely matched to reduce turbidity to acceptable levels. For the plain PMMA particles this is achieved by using a mixture of solvents, whereas for the copolymer particles, refractive index matching is achieved by suspending in a single solvent cis-decalin (n = 1.483 at 25°C).[30]

Particle Fractionation

The purpose of these procedures is to prepare particles with subtle differences in polydispersity by starting with the original stock solution of each particle type (designated A), and subjecting them to careful fractionation by centrifugation. For larger particles (R>1000nm), each fractionation step consisted of suspending a small amount of the particle suspension in dodecane (volume fraction around 5%) in 100ml centrifuge tubes. Several identical samples were prepared. The samples were then centrifuged under such conditions that particles of the mean diameter sedimented approximately ¾ of the filling height (600 RPM (~60g in the middle of the sample) for 6 minutes at 25°C). The samples

were then carefully removed from the centrifuge, and the supernatant removed by aspiration. The small plug of particles at the bottom of the tube was then re-suspended in the solvent. Some of these particles were kept aside, and the others were subjected to a repeated fractionation. The results of each fractionation step were labelled alphabetically (A, B, C...).

For smaller particles (R~200nm), the first fractionation step was similar, except the particles dispersed in dodecane at a volume fraction of ~3%. Four identical samples were prepared in 100ml centrifuge tubes and were centrifuged at a speed of 1150 rpm (~220g) for 30 min at 25°C. The samples were then carefully removed from the centrifuge, and the supernatant was removed very carefully using a pipette. The small plug of particles at the bottom of the tube was then re-suspended in the solvent. A third of these particles were kept aside, and the others were subjected to a repeated fractionation.

In the second fractionation step the particles were prepared in separate tubes in dodecane at a volume fraction of 20%. 28ml centrifuge tubes were filled with 26ml decalin, then 2ml of the particle suspension was carefully layered on top of the decalin, resulting in a total filling height of 90mm. These samples were centrifuged at 1300 rpm (~280g) for 15 min at 25°C. Following centrifugation, the first 20mm of the suspension was removed. The next 55mm was then removed, and half of it was kept and the other half was used for the final fractionation step. The lowest 15mm were also redispersed, but never used. The final fractionation step was similar to the second one, except centrifugation time was 13 min. The upper 85mm was removed and only the lowest 5mm of the suspension was kept.

The particle suspensions used, along with their radii, polydispersities, symmetry and designation, are shown in Table 1.

Scanning Electron Microscopy (SEM)

The major advantage of particle size determination by SEM is that it provides high resolution information about both particle size and shape. The major disadvantage is that the particle images need to be individually measured – in other words SEM is a particle counting technique, which produces a number-weighted size distribution. Size and shape can be accurately assessed, but only for a relatively

small population of particles on a single image (a few tens to a few hundred at best). By comparison, most ensemble techniques (e.g. light scattering) sample thousands or tens of thousands of particles simultaneously. The determination of PSDs using SEM is thus limited by counting statistics, and the challenge is to image and measure a sufficiently large number of particles to obtain a statistically acceptable PSD. In this paper we report on the results of manual counting from SEM images. A comparison with a number of automatic counting methods will be presented elsewhere (Marnette et al., in preparation).

To prepare samples for the SEM, glass microscope slides (75x25x1mm^3, Superior Marienfeld GmbH) were used as substrates. The substrates were first pre-cleaned with ultrapure water and Decon90 before cleaning them with hot sulphuric acid for 12 hours. Then they were rinsed with ultra pure water and dried under a stream of nitrogen. The wettability of the substrates was kept constant by this cleaning procedure and was checked measuring the meniscus height when the substrate was dipped vertically in decalin. A set of test experiments was carried out to optimize the conditions for reproducible sample preparation. Therefore a 40μl drop of decalin was placed in the centre of the slide and was spread out to squares of different areas up to 1200mm^2 in size using a pipette tip. The samples were placed in a saturated decalin atmosphere to determine which drop sizes were the most stable. The optimal size was found to be 660mm^2.

In preparing the samples for the SEM investigation the volume fraction of the suspensions was adjusted to obtain a sparse monolayer (about 5 times lower packing than a dense packed monolayer) after drying. 40μl of the suspension was placed on the glass slide and a rectangular drop of 660mm^2 was prepared. The sample was directly transferred onto a horizontally adjusted tilting platform which was placed inside a dust free cabinet. The sample was dried at (25±0.5)°C. In that way homogeneous films could be obtained and local segregation during drying could be avoided. The dried samples were covered with a gold layer of 5 nm thickness using an SPI sputter coating system. SEM was carried out on a FEI Quanta 200 Environmental Scanning Electron Microscope (voltage: 30 kV, pressure: 0.5-0.6

torr, magnification: x2500-x30000, spot size 3-4 (corresponding to ~10-20nm). Prior to recording images, care was taken that the images were of regions where there was no obvious particle segregation or clumping. Between 9 and 15 images were taken at different positions on the sample, and all images were used in the analysis. Figure 1 shows a typical SEM image used for analysis.

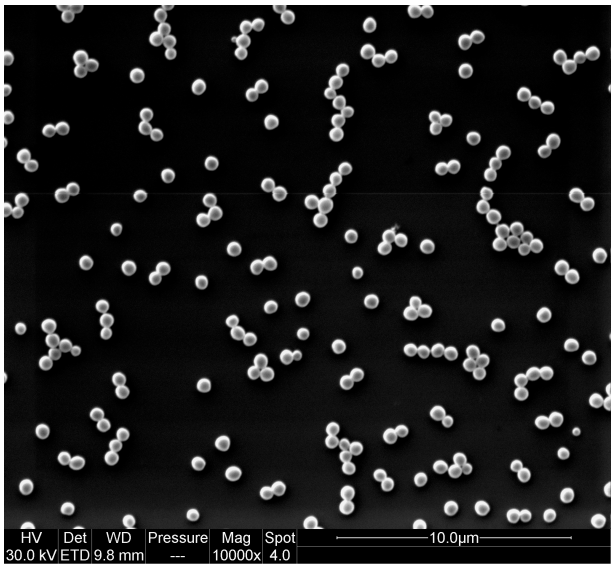

Figure 1. Typical SEM picture used for PSD determination (XL65-A)

SEM artefacts

There are a number of possible sources of error which may bias PSD determination using SEM. First is the possibility of size segregation during sample preparation, illustrated in figure 2a. Such segregation can lead to heterogeneous deposition, especially in regions where dewetting of the substrate occurs during the drying process (due to retraction of a contact line, dragging particles along with it). Second, there is the difficulty in accurately measuring particle size if particles are touching and/or overlapping in the images, as illustrated in figure 2b. Ideally particles should be well dispersed in a monolayer on the substrate surface, and should be clearly separated from each other. Nevertheless, specimens formed by drying of a polydisperse dilute suspension onto a planar substrate, even carefully prepared, always contain agglomerates that form during the drying process (in plane capillary attraction tends to stick particles together). Single small particles touching with larger ones can be partially hidden, making image analysis difficult. Similar sized particles touching (as in figure 1) is not such a large problem.

Another potential problem is damage due to electronic irradiation, leading to particle melting and misleading particle sizes (illustrated in figure 2c). Care must be taken to irradiate an area for as short a time as possible. Finally there are a number image distortions (blurring, low contrast, noise) which can affect automatic particle size determination (discussed elsewhere), but are less critical if manual counting is carried out. For a detailed discussion see.[31]

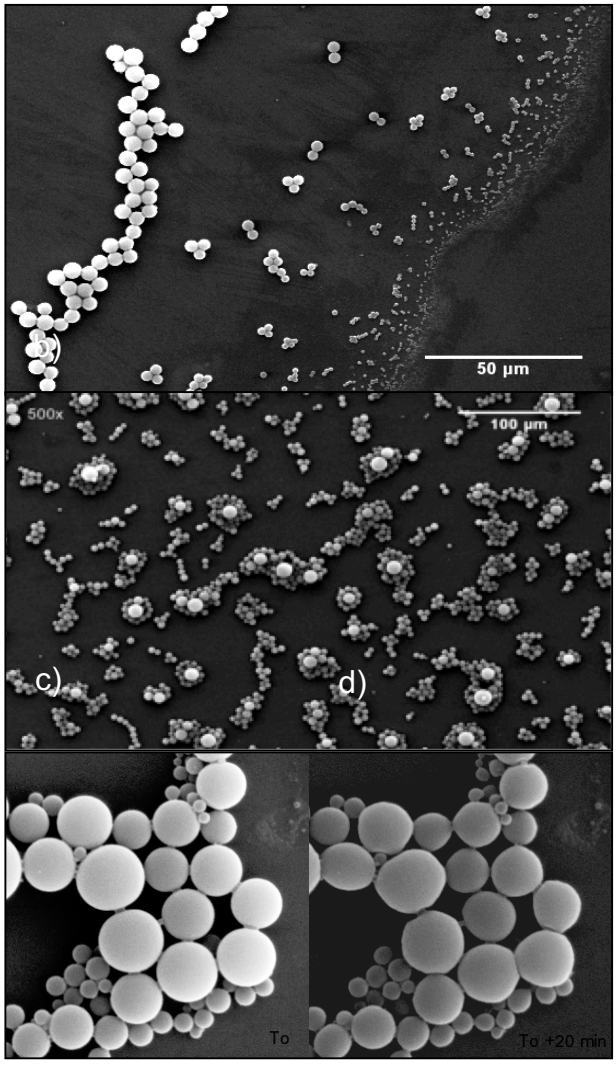

Figure 2. Illustrates a number of artefacts which must be avoided for accurate PSD determination. A very polydisperse sample (designated W9) is used to highlight these effects. (a) shows particle segregation during the drying process, with poor wettability of the substrate and radial retraction of the droplet during the drying process. The larger particles are dragged toward the heart of the liquid during drying. (b) shows agglomerates of particles due to capillary effects: small particles collapsing around

large ones. Image analysis of such an image is very difficult. See figure 4 for explanation. (c,d) shows particle damage due to SEM irradiation (melting), which induces surface melting of the particles. Image on the right was taken after ~20 min scanning, with an accelerating voltage of 3 kV, a spot size of 4.5, and a magnification of 4000x. For a detailed discussion and explanation of these effects see.[31]

To determine the PSD, the images obtained by SEM were printed on a poster printer on A0 paper so that each particle was not smaller than 10mm. Each particle diameter was measured four times in different orientations using a digital calliper. To obtain a reference measurement a test image was generated consisting of 100 images of the same particle, arranged randomly as isolated particles, doublets, triplets and so on. All measured PSDs were deconvoluted using this measurement to reduce instrumental uncertainty.

Static and Dynamic Light Scattering

The method introduced by Pusey and van Megen,[26] and further refined recently,[27] overcomes one of the main difficulties of using DLS to measure the PSDs of particles with small polydispersity. The method exploits the variation in the optically weighted scattering intensity of the diffusion coefficient as the minimum in the particle form factor is traversed. The method is explained only briefly here.

Consider a suspension of particles with a normalized PSD, (i.e. the number of particles as a function of radius), G(R). The intensity, I(q), of light scattered by the suspension as a function of the scattering vector $q = \frac{4\pi n}{\lambda}\sin(\theta)$, is given by the convolution of the PSD with the radius dependent form factor P(q,R):[26]

$$I(q) = \int_0^\infty R^6 P(q,R) G(R) dR \qquad (1)$$

where n is the refractive index of the solvent, and λ is the wavelength of the scattering light in vacuo. Analogous to Eq. (1), the effective, intensity weighted diffusion coefficient, $D_e(q)$ is expressed as:

$$D_e(q) = \frac{\int_0^\infty R^6 P(q,R) D(R) G(R) dR}{I(q)} \quad (2)$$

where the diffusion coefficient for a particular radius, R, is given by:

$$D(R) = \frac{kT}{6\pi\eta R} \quad (3)$$

where kT is the thermal energy and η is the solvent viscosity. $D_e(q)$ is obtained from the time auto-correlation function of the scattered intensity by the standard method of cumulants.[32] For a polydisperse system, the apparent radius is thus a function of angle. This is due to the fact that the form factor minimum occurs at different angles for different particle radii. Thus, for a polydisperse system, as the form factor minimum is traversed, the apparent radius drops, and then rises as first the larger, and then smaller, particles pass through their form factor minimua. This characteristic shape can be fitted to yield the PSD.

Thus both Dynamic and Static Light Scattering can be used to provide estimates of the PSD, by fitting equations 1 and 2 to the experimental data. In practice this is done by assuming a particular PSD, fitting to the experimental data, then adjusting the parameters until the best agreement is obtained between I(q) and $D_e(q)$, numerically evaluated by Eq. (1) and (2), and the corresponding measured quantities. The PSD can be an arbitrary shape, and we have implemented fitting routines for Gaussian, Log-Normal and Weibull distributions,[27] as well as for a discrete, user defined distribution. Details of these and other PSDs, that could equally well be considered, may be found in standard statistical texts.

The PSD is constructed by dividing an appropriate radius range into one thousand bins. For each radius, intensity form factors are calculated using Mie theory, and then summed over the distribution. For a chosen distribution, the simulated results are compared with the experimental values, and a least squares fit is performed. The analysis was carried out in an in-house program written in MATLAB, with the Mie calculations based on the FORTRAN algorithm "BHMIE" of Bohren and Huffman.[33]

All measurements were performed with an ALV TCDLS spectrometer (ALV GMBH, Germany),[34]

and the methods used here been described previously.[28] The minimum dwell time at each angle in the range $20° \leq \theta \leq 120°$ was 180s, and the measurements at each angle are the average of 3 repeat measurements.

Results & Discussion

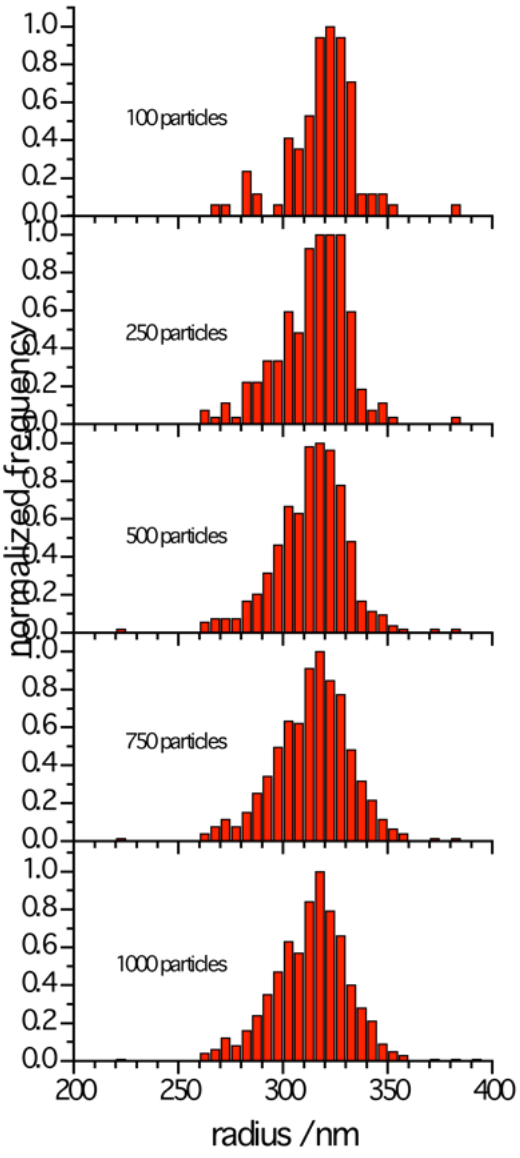

Figure 3. Particle size distributions for XL65-C, as a function of the number of particles measured.

Particle diameters were measured manually, as outlined in the text. The figure demonstrates that a minimum of 500 particles are needed to approximate the true PSD.

Figure 3 shows the results of manual measurement of particle size from SEM results. As can be seen, the PSD is not well determined until of the order of 500 particles are counted. PSDs determined using fewer particles could have statistical artefacts. In order to generate good statistics, it is also necessary to take micrographs at several different positions within the sample. The results shown are taken at a magnification of 10000x, with approximately 50 to 200 particles in the field of view. A typical SEM image is shown in figure 1. 9 to 15 independent images are analysed to provide the final 1000 particle result.

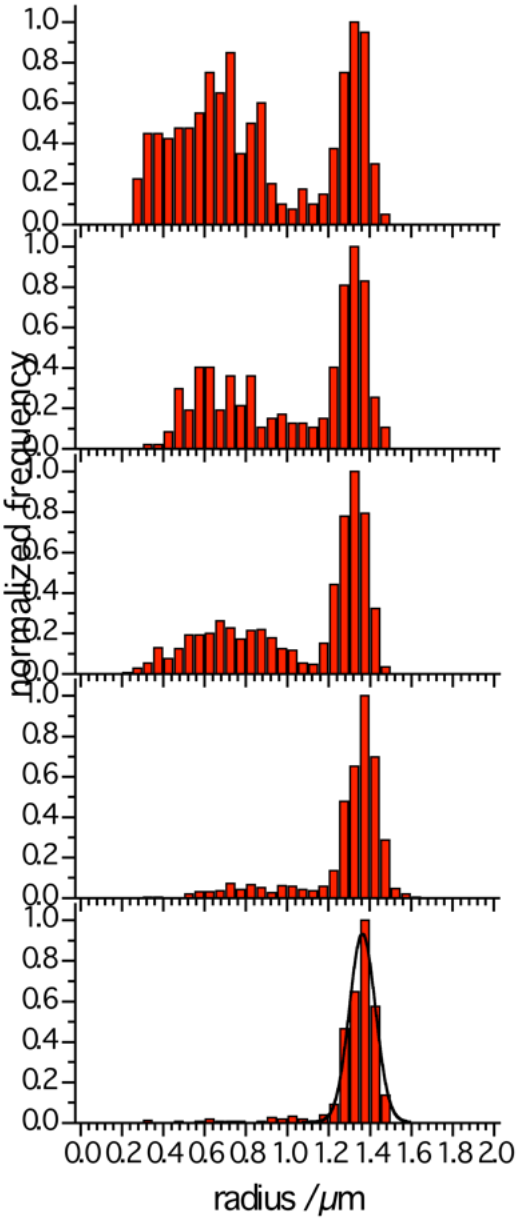

Figure 4. The figure shows 5 successive fractionations of SMU23, a large, very broad multimodal particle size distribution. The final distribution is almost Gaussian. Measurements were made manually from SEM images as described in the text.

Having established a reliable protocol for the accurate determination of the PSD, figure 4 shows the effects of fractionation on the PSDs, determined by electron microscopy of about 600 particles, for a micron sized bimodal distribution (designated SMU23). Starting with very broad multimodal distributions we obtained a narrow, almost Gaussion distribution after four fractionation steps. The fit

parameters for the final fractionation are given in table 1.

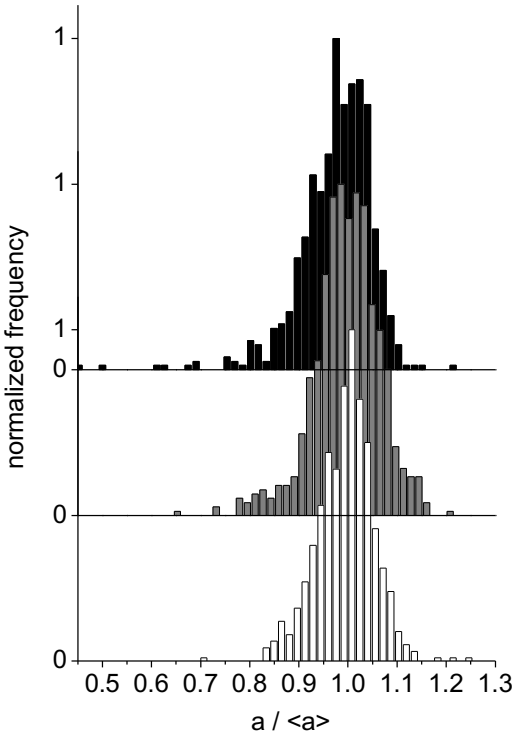

Figure 5. Effect of fractionation on the PSD for XL65 particles. Results are from manual counting of about 1000 particles.

The technique is not, however, restricted to converting a bimodal distribution to a mono-modal one. Figure 5 shows similar data for sub-micron sized particles (designated XL65), again from about 1000 particles. Starting with a skewed distribution with a polydispersity (defined as $\sigma(a)/\langle a \rangle$) of 5.8% (XL65-A), in the two fractionation steps the width and the skewness of the distribution is reduced leading to a skewed distribution with 5.3% (XL65-B) and finally to an almost symmetric distribution with 4.8% (XL65-C). All results are summarized in Table 1. As can be seen from figures 4 and 5 it is possible to decrease the polydispersity of the sample significantly as well as to change slightly the shape of the PSD using the presented fractionation method.

Particle	Composition	Radius (± 7 nm)	Polydispersity (±0.25%)	Shape

XL65-A	PMMA/TFEA	320 nm	5.8%	Negatively Skewed
XL65-B	PMMA/TFEA	320 nm	5.3%	Slightly skewed
XL65-C	PMMA/TFEA	320 nm	4.8%	Gaussian
SMU23-E	PMMA	1360 nm	4.9%	Gaussian

Table 1. Particle size distribution characteristics for the particles shown in this paper.

Figure 6 shows the measured form factors for XL65 particles before fractionation. The continuous curves are the best fit curves assuming a Weibull distribution. Similar results were obtained using Gaussian or log-normal distributions. Also shown are the form factors calculated by using the PSD determined from SEM.

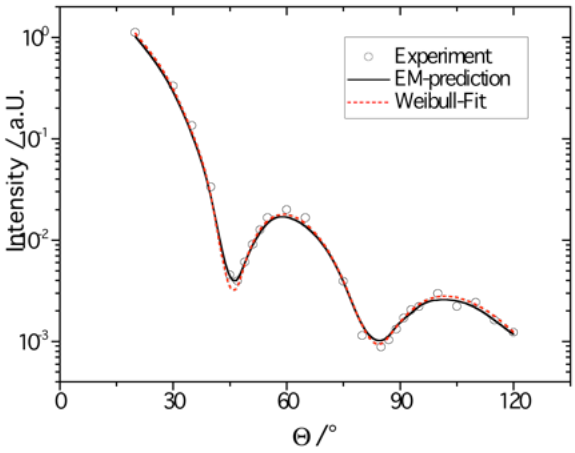

Figure 6. shows the intensity form factor, as measured by Static Light Scattering for XL65-A. The best fit using a negatively skewed (Weibull) distribution (dotted line) fits reasonably well. However a better fit is obtained by using the measured PSD from SEM to calculate the form factor.

Figure 7 represents the apparent radius as a function of the scattering angle around the first minimum of the form factor for XL65-A. The data follow the behaviour described above. The dotted and dashed curves are the best fits to the radius and intensity date respectively, using a Weibull distribution, whereas the solid line represents the prediction calculated using the PSD obtained in SEM measurements.

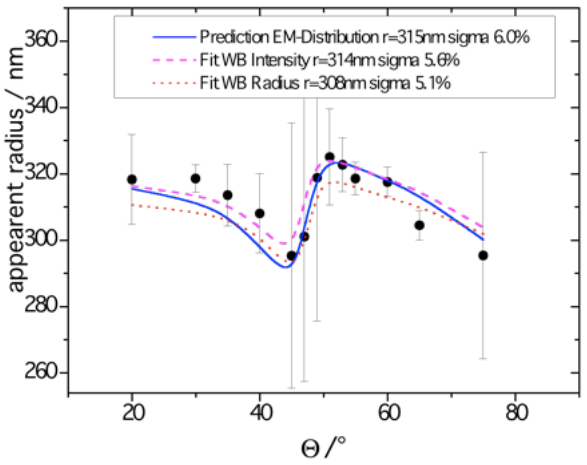

Figure 7. shows the apparent radius, as determined by Dynamic Light Scattering, as a function of angle. Each point represents the average and standard deviation of 3 measurements. The dotted line is the best fit to the radius data, and the dashed line is the best fit to the intensity data (figure 7), using the method described in,[27] illustrating the relatively sensitivity of the technique. However the agreement is further improved by using the PSD determined from SEM (solid line). These results demonstrate that the PSDs determined by SEM light scattering are in good agreement. Note that error bars are very large in the region of the form factor minimum due to the very low intensity in this region.

As can be seen, in both cases the best fits and the SEM results are comparable. This shows that the SEM results are robust, and are consistent with the LS results. It also illustrates that the SEM is sensitive to the very small changes in polydispersity we observe in these samples.

Conclusions

We have shown that subtle changes in both the shape of the particle size distribution, and the overall polydispersity, can be achieved using fractionation. We have conducted a thorough analysis of the use of SEM for the characterization of the particle size distribution, and shown that at least 500-1000 particles must be measured in order to accurately characterize the PSD. We have demonstrated the importance of sample preparation and segregation during drying. Finally, we have shown that the SEM

results are consistent with those of static and dynamics light scattering. However, the light scattering less sensitive to very small changes in the PSD. In situations where the details of the PSD are important, both methods should be used.

HJS would like to thank the Alexander von Humboldt Foundation for providing financial support. This project is proudly supported by the International Science Linkages established under the Australian Government's innovation statement, Backing Australia's Ability.

SYNOPSIS TOC

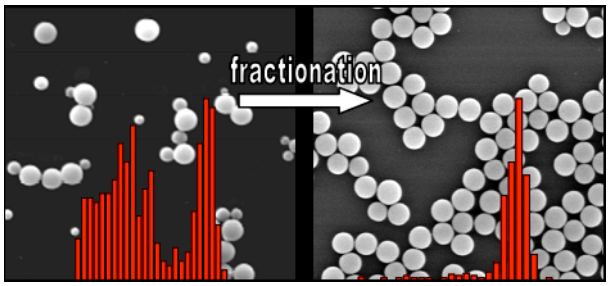

REFERENCES

(1) Pusey, P. N.; van Megen, W. *Nature (London)* **1986,** 320, 340-342.
(2) Ackerson, B. J. *Phase Transitions, Secial Issue: Phase Transitions in Colloidal Suspensions* **1990,** 21, (2-4), 73-250.
(3) Zahn, K.; Lenke, R.; Maret, G. *Physical Review Letters* **1999,** 82, (13), 2721-2724.
(4) Pham, K. N.; Egelhaaf, S. U.; Pusey, P. N.; Poon, W. C. K. *Physical Review E* **2004,** 69, 011503.
(5) Poon, W. C. K. *Journal of Physics: Condensed Matter* **2002,** 14, R859-R880.
(6) Sugimoto, T. *Monodispersed Particles*. First ed.; Elsevier: Amsterdam, 2001.
(7) Auer, S.; Frenkel, D. *Nature (London)* **2001,** 413, 711-713.
(8) Henderson, S. Crystallisation From the Melt. A Study of Polydisperse Hard Sphere Colloids. Ph.D, Royal Melbourne Institute of Technology, Melbourne, 1999.
(9) Bartlett, P. *Journal of Physics: Condensed Matter* **2000,** 12, A275-A280.
(10) Evans, R. M. L.; Holmes, C. B. *Physical Review E* **2001,** 64, (1), 1404-1412.
(11) Martin, S.; Bryant, G.; van Megen, W. *Physical Review E* **2003,** 67, 061405.
(12) Martin, S.; Bryant, G.; van Megen, W. *Physical Review E* **2005,** 71, 021404.
(13) Williams, S. R.; Snook, I. K.; van Megen, W. *Physical Review E* **2001,** 64, (2), 1506-1512.
(14) Williams, S.; McGlynn, P.; Bryant, G.; Snook, I. K.; van Megen, W. *Physical Review E* **2006,** 74, 031204.
(15) Williams, S.; Bryant, G.; Snook, I. K.; van Megen, W. *Physical Review Letters* **2006,** 96, 087801.
(16) Schöpe, H. J.; Bryant, G.; van Megen, W. *Physical Review Letters* **2006,** 96, 175701.
(17) Schöpe, H. J.; Bryant, G.; van Megen, W. *Physical Review E* **2006,** 74, 060401(R).
(18) Martin, S.; Bryant, G.; van Megen, W. *Physical Review Letters* **2003,** 90, 255702.
(19) Schall, P.; Spaepen, F. *International Journal of Materials Research* **2006,** 97, (7), 958-962.
(20) Schöpe, H. J. *Journal of Physics: Condensed Matter* **2003,** 15, L533-L540.
(21) Barth, H. G.; Flippen, R. B. *Analytical Chemistry* **1995,** 67, (12), R257-R272.
(22) Bott, S. E. *Particle Size Analysis* **1988**, 77-89.
(23) Bryant, G.; Thomas, J. C. *Langmuir* **1995,** 11, (7), 2480-2485.
(24) Bryant, G.; Abeynayake, C.; Thomas, J. C. *Langmuir* **1996,** 12, 6224-6228.
(25) Vega, J. R.; Gugliotta, L. M.; Gonzalez, V. D. G.; Meira, G. R. *Journal of Colloid and Interface Science* **2003,** 261, 74-81.
(26) Pusey, P. N.; van Megen, W. *Journal of Chemical Physics* **1984,** 80, (8), 3513-3520.
(27) Bryant, G.; Martin, S.; Budi, A.; van Megen, W. *Langmuir* **2003,** 19, 616-621.
(28) Bryant, G.; Mortensen, T.; Henderson, S.; Williams, S.; van Megen, W. *Journal of Colloid and Interface Science* **1999,** 216, 401-408.
(29) Bryant, G.; Williams, S. R.; Snook, I. K.; LinMao, Q.; Perez, E.; Pincet, F. *Physical Review E* **2002,** 66, 060501(R).
(30) Underwood, S. M.; van Megen, W. *Colloid and Polymer Science* **1996,** 274, 1072-1080.
(31) Marnette, O. A Videomicroscopic study of crystallization in polydisperse 2D hard spheres. PhD, Université Paris VI, Paris, 2007.
(32) Brown, J. C.; Pusey, P. N.; Dietz, R. *Journal of Chemical Physics* **1975,** 62, (3), 1136-1144.
(33) Bohren, C. F.; Huffman, D. R. *Absorption and Scattering of Light by Small Particles*. Wiley: New York, 1983.
(34) Segre, P. N.; van Megen, W.; Pusey, P. N.; Schätzel, K.; Peters, W. *Journal of Modern Optics* **1995,** 42, (9), 1929-1952.